Ground and Excited-State Performance of an Quantum-Dot Semiconductor Amplifier

Benjamin Lingnau, Eckehard Schöll, and Kathy Lüdge
Technische Universität Berlin, Institut für Theoretische Physik

***Abstract*—Using an optimized delay-differential-equation model, we efficiently simulate the signal propagation through a quantum-dot semiconductor amplifier. We analyze the device performance by means of the signal quality factor when amplifying signals on either the ground or excited state transition, in dependence of pump current and signal power.**

I. Introduction

Quantum-dot semiconductor optical amplifiers (QDSOAs) are potential candidates for use in high bit-rate optical data communication, due to the fast scattering of charge carriers in a carrier reservoir into the optically active quantum-dot (QD) states [1]. The broad amplification spectrum of QDs due to inhomogeneous broadening and the existence of excited state transitions potentially allows the amplification of signals over a broad range of wavelengths. In this work we explore this possibility and investigate the device performance on ground state (GS) and excited state (ES) wavelengths to explore optimal operation conditions.

II. Model

We consider a 3 mm long QDSOA device with a $4\,\mu$m wide ridge waveguide structure, with an active medium consisting of $a_L = 10$ InGaAs quantum-well (QW) layers (thickness $h^{QW} = 5\,$nm), each embedding a density of $N^{QD} = 3.5 \times 10^{10}\,\mathrm{cm}^{-2}$ InAs QDs. The energy structure across one QD is sketched in Fig. 1. We describe the QDSOA device using a delay differential equation (DDE) approach [2]. We discretize the device along the propagation axis z into 31 equally spaced points along the device. The slowly varying electric field amplitude of the forward and backward propagating wave $E_\pm(z,t)$ is then given by

$$E_\pm(z,t) = e^{\frac{\Delta t}{2}[g(z,t)+g(z\mp\Delta z,t-\Delta t)]} E_\pm(z\mp\Delta z, t-\Delta t) + \eta(z,t)\,, \tag{1}$$

where Δz is the distance between space discretization points, and $\Delta t = \Delta z / v_g$ is the corresponding propagation time, with v_g the group velocity, and $\eta(z,t)$ is a colored noise source term, describing spontaneous emission. The amplitude gain $g(z,t)$ is determined from the material equations for electrons and holes (denoted by $b \in \{e,h\}$) evaluated at each space discretization point:

$$\frac{\mathrm{d}}{\mathrm{d}t} w_b = J - r^w_{loss}(w_e,w_h) - 2N^{QD}\sum_{j,m} f(j)\nu_m S^{cap,j}_{b,m} \tag{2}$$

$$\frac{\mathrm{d}}{\mathrm{d}t}\rho^j_{b,m} = -W_m\rho^j_{b,m} + S^{cap,j}_{b,m} + S^{rel,j}_{b,m} - \mathrm{Re}\left(g^j_m\right)\left(|E_+|^2 + |E_-|^2\right) \tag{3}$$

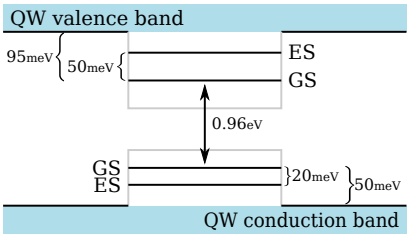

Fig. 1. Sketch of the energy structure across one QD within the QDSOA.

Here, w_b is the charge carrier 2D density in each QW layer, with J being the pump current density per layer, and $r^w_{loss}(w_e,w_h) = A^S\sqrt{w_e w_h} + B^S w_e w_h$ describing linear and bimolecular carrier losses. The QDs are distributed into subgroups with different transition energies in order to account for the inhomogeneous broadening, labeled by the index j, while the localized QD state is denoted by $m \in \{GS, ES\}$, with their degeneracy (excluding spin) ν_m. We assume Gaussian probability distributions $f(j)$ around the respective central wavelength with a FWHM of 28meV for the GS and 42meV for the ES. The QD occupation probabilities $\rho^j_{b,m}$ are coupled to the QW by charge scattering:

$$S^{cap,j}_{b,m} = S^{cap,j,in}_{b,m}\left(1-\rho^j_{b,m}\right) - S^{cap,j,out}_{b,m}\rho^j_{b,m}\,, \tag{4}$$

$$S^{rel,j}_{b,m} = \pm\frac{1}{\nu_m}\left[S^{rel,j,in}_b\left(1-\rho^j_{b,GS}\right)\rho^j_{b,ES} - S^{rel,j,out}_b\rho^j_{b,GS}\left(1-\rho^j_{b,ES}\right)\right], \tag{5}$$

where S^{cap} describe direct capture or escape processes between QD and QW states, and S^{rel} are intra-dot relaxation processes ($+$ for GS, $-$ for ES). The respective in and out-scattering rates are microscopically calculated in dependence of QW charge carrier density and temperature [3].

The stimulated emission coefficient for each QD subgroup is given by

$$g^j_m = \frac{|\mu_m|^2 T_2^m}{2\hbar^2}(\rho^j_{e,m} + \rho^j_{h,m} - 1)\frac{1 - i\Delta\omega^j_m T_2^m}{1 + (\Delta\omega^j_m T_2^m)^2}\,, \tag{6}$$

where $\Delta\omega^j_m = \omega^j_m - \omega$ is the frequency detuning between the transition of the corresponding subgroup and the optical wavelength, T_2^m and μ_m are the dephasing time and the optical dipole moment for the m-th state. The total complex optical gain is then given by

$$g(z,t) = \Gamma\frac{\hbar\omega}{2\varepsilon_{bg}\varepsilon_0}\frac{2N^{QD}}{h^{QW}}\sum_{j,m}\nu_m f(j) g^j_m(z,t)\,, \tag{7}$$

with the optical confinement factor Γ and the background permittivity ε_{bg}.

978-1-4799-3682-3/14/$31.00 ©2014 IEEE

TABLE I. PARAMETERS USED IN THE SIMULATIONS.

symbol	value	symbol	value
A^S	$0.6\,\mathrm{ns}^{-1}$	W_{GS}	$0.45\,\mathrm{ns}^{-1}$
B^S	$50\,\mathrm{nm}^2\,\mathrm{ns}^{-1}$	W_{ES}	$0.60\,\mathrm{ns}^{-1}$
T_2^{GS}	$200\,\mathrm{fs} \times (1 + \frac{j}{150\mathrm{mA}})^{-1}$	μ_{GS}	$0.55 e_0$ nm
T_2^{ES}	$300\,\mathrm{fs} \times (1 + \frac{j}{150\mathrm{mA}})^{-1}$	μ_{ES}	$0.62 e_0$ nm
ε_{bg}	14.2	Γ	0.06

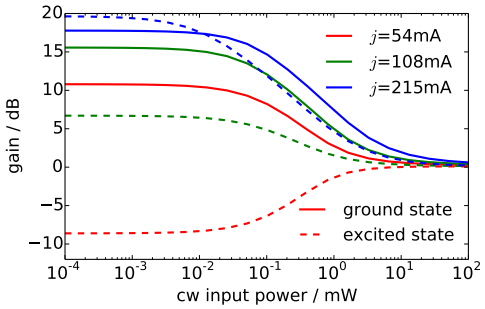

Fig. 2. Gain saturation characteristics of the QDSOA device. Shown is the device gain of an optical cw signal in dependence of its input power for different currents j. The signal is either centered on the GS (solid lines) or the ES (dashed lines).

III. RESULTS

We simulate the QDSOA with parameters given in Tab.1. We introduce a phenomenological dependence of the dephasing times on the current, obtained from fits to experimental data, as well as a temperature dependence $T = 295\,\mathrm{K} + j \times 0.1\,\mathrm{K\,mA}^{-1}$, where $j = \eta J A a_L$ is the pump current, with an injection efficiency $\eta = 0.5$ and the device area A.

A characterization of the gain properties of the device is shown in Fig. 2 for different pump currents in dependence of the optical cw input power. With increasing current, a saturation of the GS gain can be observed, whereas the ES gain continues to increase and surpasses that of the GS at around 200 mA. The ES transition therefore potentially offers a greater gain than the GS. However, the ES also shows a stronger gain compression with increasing input optical power, i.e., the device is unable to provide a high gain once the input signals become too strong, thus limiting the operation on the ES to smaller optical power.

We now consider pseudo-random optical on-off-keyed bit-signal patterns at a repetition rate of $40\,\mathrm{Gb\,s}^{-1}$ as input to the amplifier, with varying average power. We evaluate the amplification performance in terms of the quality factor Q:

$$Q = \frac{\langle I \rangle_{on} - \langle I \rangle_{off}}{\sigma_{on} + \sigma_{off}}\,, \tag{8}$$

where $\langle I \rangle_{on/off}$ is the average output intensity of the one or zero-bit, respectively, and $\sigma_{on/off}$ is the corresponding variance of the output intensity level.

Figure 3 shows the Q-factor for GS and ES amplification in dependence of the average input signal power. The insets show the corresponding eye-diagrams of the output signal, created by overlaying the whole time-series of the output intensity within an interval of three bits. A high quality factor corresponds to clearly distinguishable zero and one-bits of the output signal.

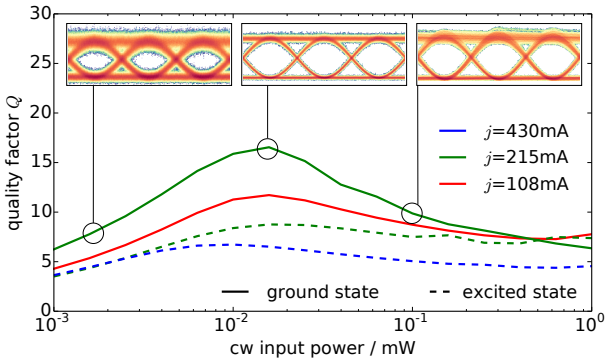

Fig. 3. Quality factor of an amplified pseudo-random bit sequence on the GS (solid) or the ES (dashed), for different pump currents. The insets show representative eye-diagrams of the amplified output GS bit-pattern corresponding to the circled data points.

An optimum value of the input power can be seen [4], limited by noise at smaller signal strengths, and the onset of nonlinear patterning effects at higher intensities. With higher currents, the optimum Q-factor increases for the GS due to the saturation of the GS gain along with increased scattering rates, refilling the GS more efficiently and suppressing patterning effects. The ES on the other hand shows a decrease of the optimum with increasing current, owed to the more efficient coupling of the ES population to the QW carrier reservoir. The stronger response of the slow QW population then lead to pronounced patterning effects.

IV. CONCLUSION

We have analyzed the amplification performance of a QDSOA for operation on the ground or excited state. Both GS and ES show an optimum input power of optical signals, given by the interplay of noise and patterning effects. The operation on the GS shows generally a better performance than on the ES, attributed to the fast carrier relaxation from ES to GS states, whereas only the QW acts as a carrier reservoir for ES states.

ACKNOWLEDGMENT

This work was supported by DFG within Sfb787.

REFERENCES

[1] D. Bimberg, G. Fiol, M. Kuntz, C. Meuer, M. Lämmlin, N. N. Ledentsov, and A. R. Kovsh, "High speed nanophotonic devices based on quantum dots," *phys. stat. sol. (a)*, vol. 203, no. 14, pp. 3523–3532, 2006.

[2] J. Javaloyes and S. Balle, "Multimode dynamics in bidirectional laser cavities by folding space into time delay," *Opt. Express*, vol. 20, no. 8, pp. 8496–8502, 2012.

[3] N. Majer, S. Dommers-Völkel, J. Gomis-Bresco, U. Woggon, K. Lüdge, and E. Schöll, "Impact of carrier-carrier scattering and carrier heating on pulse train dynamics of quantum dot semiconductor optical amplifiers," *Appl. Phys. Lett.*, vol. 99, p. 131102, 2011.

[4] S. Wilkinson, B. Lingnau, J. Korn, E. Schöll, and K. Lüdge, "Influence of noise on the signal properties of quantum-dot semiconductor optical amplifiers," *IEEE J. Sel. Top. Quantum Electron.*, vol. 19, no. 4, p. 1900106, 2013.